

# Effect of the Structure at the Micrometer and Nanometer Scales on the Light Transmission of Isotactic Polypropylene

Qamer Zia, René Androsch, Hans-Joachim Radusch

Center of Engineering Sciences, Martin Luther University of Halle-Wittenberg, 06099 Halle/Saale, Germany

Received 16 April 2009; accepted 21 October 2009

DOI 10.1002/app.31638

Published online 26 March 2010 in Wiley InterScience (www.interscience.wiley.com).

**ABSTRACT:** The spherulitic superstructure, crystallinity, and structure and morphology of crystals of isotactic polypropylene were controlled by the conditions of melt crystallization and related to the transmittance of visible light. Spherulitic samples, which contained monoclinic lamellae, were prepared by slow cooling of the quiescent melt at rates lower than 10 K/s and by isothermal melt crystallization at temperatures between 373 and 413 K. Nonspherulitic specimens, which contained nonlamellar mesomorphic domains, in contrast, were obtained by rapid cooling of the melt with rates faster than 100 K/s. The crystallinity and the size of crystals were furthermore fine-tuned by subsequent annealing at elevated temperatures. Analysis of such films of different structure

by ultraviolet–visible spectroscopy revealed that the light transmission was independent of (1) the fraction, (2) the internal structure, and (3) the size of the crystals. In contrast, the light transmission increased with decreasing size of spherulites and finally exceeded 90% in films of 100  $\mu\text{m}$  thickness when spherulites were completely absent. The crystallinity and the structure and size of the crystals of the films of isotactic polypropylene could be adjusted within wide limits without affecting the light transmission. © 2010 Wiley Periodicals, Inc. *J Appl Polym Sci* 117: 1013–1020, 2010

**Key words:** isotactic; poly(propylene) (PP); structure; transparency; UV-vis spectroscopy

## INTRODUCTION

Isotactic polypropylene (iPP) is a semicrystalline and polymorphic thermoplastic. Crystals of different structures and morphologies can be generated by variation of the conditions of crystallization.<sup>1–5</sup> A spherulitic superstructure with monoclinic lamellae and an amorphous phase develops on isothermal crystallization at temperatures higher about 350 K or on slow cooling of the melt at rates lower than about 10<sup>2</sup> K/s.<sup>6–8</sup> In contrast, a nonspherulitic superstructure with nodular mesomorphic domains with a size of about 10–20 nm and an amorphous phase forms on quenching the liquid to ambient temperature at rates higher than 10<sup>2</sup> K/s.<sup>8,9</sup> The heating of these mesomorphic nodular domains triggers at first a phase transition into a monoclinic structure, which starts at about 350 K. The phase transition is not connected with a change in the crystal morphology; that is, the size and habit of crystals are nearly unchanged.<sup>10,11</sup> Further heating leads then to a clas-

sical reorganization of the structure at temperatures higher than about 400 K. As a result, the size of nodules increases to about 40 nm; however, the nonlamellar habit and the nonspherulitic organization are preserved. Similarly, the annealing of spherulitic samples, which were initially crystallized at low supercooling, allows the stabilization of the monoclinic lamellae by thickening. As such, a large variety of structures at different length scales can be adjusted by the conditions of melt crystallization and subsequent annealing.<sup>8</sup>

In this study, we intended to use the unique opportunity of rather independent variation of the various parameters of structure, including crystallinity, crystal structure, crystal morphology, and higher order superstructure, to identify their effects on the optical transparency of iPP. This was a continuation of our recent efforts to gain information about structure formation at rates of cooling that typically are observed in polymer processing and about the structure–property relations of semicrystalline iPP preparations initially solidified by rapid cooling.<sup>12–14</sup>

The interaction of light with a polymer includes reflection, absorption, and scattering. Although absorption and specular reflection are negligible in the case of polymers, diffuse surface reflection and scattering may cause a reduction in the intensity of transmitted light. Diffuse reflection occurs at the

Correspondence to: H.-J. Radusch (hans-joachim.radusch@iw.uni-halle.de).

Contract grant sponsor: Deutsche Forschungsgemeinschaft.

air-polymer interface and is primarily controlled by surface roughness.<sup>15,16</sup> Major causes for surface roughness of variable length scales are melt relaxation during processing and crystallization.<sup>14,15</sup> *Scattering*, that is, a change of the direction of light, occurs at internal heterogeneities of different indices of refraction and is, in the case of semicrystalline polymers, connected to the presence of crystals and spherulites.<sup>15</sup> The angular dependence of light scattering strongly affects the optical appearance of a polymer, which often is quantified by haze. *Haze* is the intensity of scattered light at angles larger than 2.5°, which results in translucency/opacity or milky appearance of a polymer. *Transparency*, or see-through clarity, is related to the fraction of nonscattered, transmitted light required to monitor fine details of an object through a polymer film.<sup>15</sup>

Recently, a qualitative analysis of the effects of crystallinity, crystal shape/size, and superstructure on the light transmission of random propylene-1-butene copolymers was performed. It was observed that nonspherulitic films of 100  $\mu\text{m}$  thickness obtained by the quenching of the melt exhibited a transparency of about 90%. In contrast, the transparency decreased to about 50–60% in slowly cooled samples because of the presence of spherulites. Furthermore, it was found that the variation of crystallinity and the size of crystals did not largely affect the transparency. As such, it was demonstrated that samples of largely different transparencies but identical crystallinities could be generated without the use of optical clarifiers/nucleating agents.<sup>17</sup> The effect of the presence of spherulites in the polymers films on the light transmission has been evaluated in numerous fundamental publications, which all came to the conclusion that the intensity of light scattered by a spherulite is proportional to the square of its volume. Consequently, scattering is expected to increase at large scattering angles in the presence of large spherulites and to thereby reduce the light transmission in the forward direction, that is, at zero or close to zero scattering angle.<sup>18</sup>

High transparency of semicrystalline polymers is important for packaging applications and, in general, can be increased by a decrease in the size of spherulites. Technically, this is controlled either by the addition of nucleating agents or by the fast cooling of the melt.<sup>19,20</sup> A systematic study of the effects of the structure and morphology of iPP, formed in the absence of optical clarifiers/nucleating agents, through different thermodynamic pathways of crystallization on the optical properties has not yet been reported and was, therefore, the subject of this study. We were able to produce spherulitic and nonspherulitic films of different crystallinities, crystal structures, and morphologies and, even more, could control these parameters independently. In extension

of our recent investigation of the light transmission of random propylene-1-butene copolymers, we quantitatively related the light transmission of iPP films cooled at different conditions of melt crystallization to the structures and morphologies formed at the micrometer and nanometer scales.

## EXPERIMENTAL

### Material

A commercial-grade iPP from Montell Polyolefins (Bayreuth, Germany) was used in this study, which was specially produced for film-extrusion applications and the packaging industry. The mass-average molar mass and polydispersity were 373 kg/mol and 6.2, respectively. The melt flow rate was 3 g/10 min, determined at 503 K with a load of 2.16 kg.<sup>21</sup> Detailed information about the structure, density/crystallinity, and morphology of this particular grade were described elsewhere.<sup>8,12,13,22</sup>

### Film preparation

Films of iPP of 100  $\mu\text{m}$  thickness were nonisothermally crystallized between cleaned microscope glass covers in a nitrogen atmosphere at cooling rates between  $10^{-1}$  and  $10^3$  K/s with a special device for controlled rapid cooling. The description of the device and the method of film preparation were reported elsewhere.<sup>8,23</sup> Selected samples were subsequently annealed in the same device at temperatures of 393 and 433 K for a period of 60 min. In a separate preparation regime, the isothermal crystallization of films of identical thicknesses was performed in an oil bath at temperatures of 373, 383, 398, and 413 K for periods of 30, 60, 90, and 180 min, respectively. The temperature deviation was within  $\pm 1$  K. The films were carefully sealed between glass covers and aluminum foil and heated to a temperature of 473 K with a PerkinElmer film press. Samples were held at 473 K for 5 min to erase the effects of their prior thermal history. In the next step, the isothermal crystallization of the films was performed. The chosen film thickness of 100  $\mu\text{m}$  ensured minimum temperature and structural gradients, as was proven by a comparison of the bulk and surface structures with transmission electron microscopy.<sup>24</sup>

### Wide-angle X-ray scattering

Wide-angle X-ray scattering was performed to obtain information about the crystal structure of the iPP films. The data were collected on a URD 63 diffractometer from Seifert-FPM (Freiberg, Germany) with nickel-filtered Cu K $\alpha$  radiation with a wavelength of 0.15418 nm and a scintillation counter for

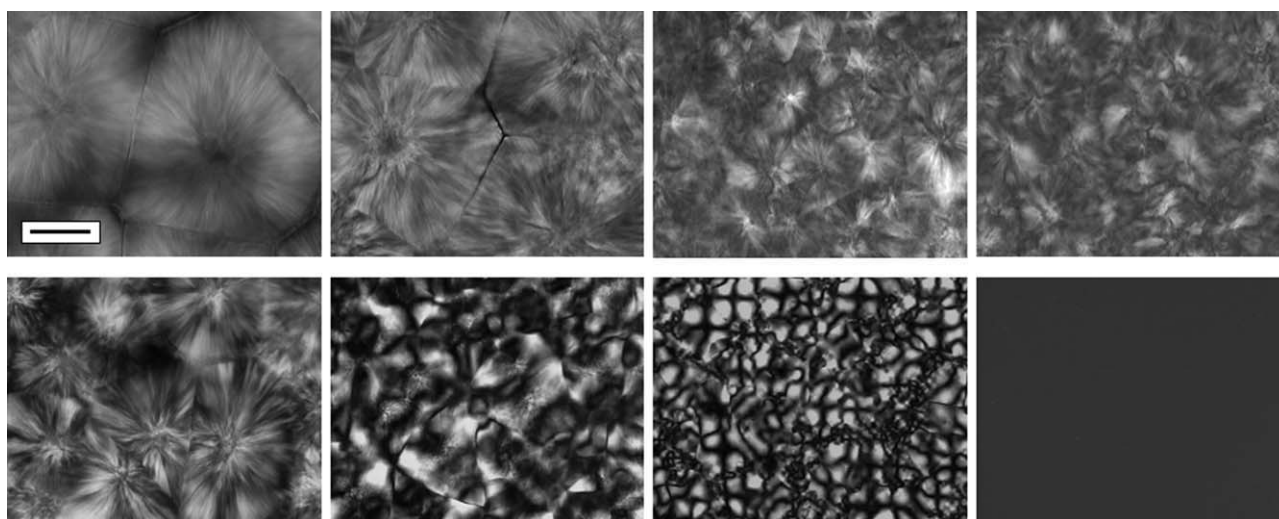


**Figure 1** Polarizing optical micrographs of 100- $\mu\text{m}$ -thick iPP films isothermally melt-crystallized (top) at 413, 398, 383, or 373 K (left to right) or nonisothermally melt-crystallized (bottom) at 0.1, 6, 12, or 450 K/s (left to right). The scale bar represents 25  $\mu\text{m}$ . Two optical micrographs in the bottom left are reproduced with permission from ELSEVIER.<sup>27</sup>

registration. Measurements were done in a symmetric transmission mode.

#### Differential scanning calorimetry (DSC)

A PerkinElmer DSC7 (Waltham, MA) was used to gain information about the crystallinity of the selected preparations. Measurements were performed at a heating rate of 20 K/min, and the crystallinity was determined from the heat of fusion of the samples. The reference value of the heat of fusion of 100% crystalline iPP, used for normalization, was 209 J/g.<sup>25</sup> The calibrations of the sensor temperature and the heat flow rate was performed according to standard procedures.<sup>26</sup>

#### Atomic force microscopy (AFM)

AFM was used for direct analysis of the morphology of the crystals. We used a universal scanning probe microscope (U-SPM, Quesant, Santa Cruz, CA), which was equipped with a  $5 \times 5\text{-}\mu\text{m}^2$  scanner. Phase images were collected at ambient temperature in tapping mode with a silicon cantilever (NSC 14, MikroMasch) with a resonance frequency and force constant of about 160 kHz and 5 N/m, respectively.

#### Polarizing optical microscopy

Information about the superstructure of the 100  $\mu\text{m}$  thick films was gained by polarizing optical microscopy in transmission mode with a Leica DMRX microscope (Wetzlar, Germany). The average size/diameter of the spherulites was estimated manually by line-intercept analysis of the spherulites in at least two images. A standard error of the mean of

about  $\pm 2\text{--}4\ \mu\text{m}$  was obtained in the size determination of the spherulites.

#### Ultraviolet–visible (UV–vis) spectroscopy

The light transmission of the iPP films was determined at ambient temperature within the visible-light wavelength range 380–750 nm with UV–vis spectrometers (Lambda 900 and Lambda 35, PerkinElmer). To account for the minor variations of the film thickness, the transparency data were normalized to a film thickness of 100  $\mu\text{m}$  with the Lambert–Beer law.<sup>14</sup> Repeated measurements of the light transmission on different samples of identical history of crystallization showed a deviation of  $\pm 2\%$ .

## RESULTS AND DISCUSSION

#### Structure at the micrometer and nanometer scales

Figure 1 shows the polarizing optical micrographs of the iPP films of 100  $\mu\text{m}$  thickness. Samples were isothermally crystallized at 413, 398, 383, and 373 K (top images, from left to right) or crystallized during cooling at rates of 0.1, 6, 12, and 450 K/s (bottom images, from left to right). The scaling bar represents a distance of 25  $\mu\text{m}$ . In general, we observed a spherulitic superstructure, with the size of spherulites decreasing with increasing supercooling, that is, decreasing temperature of crystallization. In detail, isothermal crystallization at 413, 398, 383, and 373 K led to the formation of spherulites with average sizes of 100, 75, 40, and 30  $\mu\text{m}$ , respectively. In the case of the nonisothermally crystallized samples, the spherulite sizes were 50 and 15  $\mu\text{m}$  after cooling at 0.1 and 12 K/s, respectively. Rapid cooling at a rate of 450 K/s did not result in the formation of a

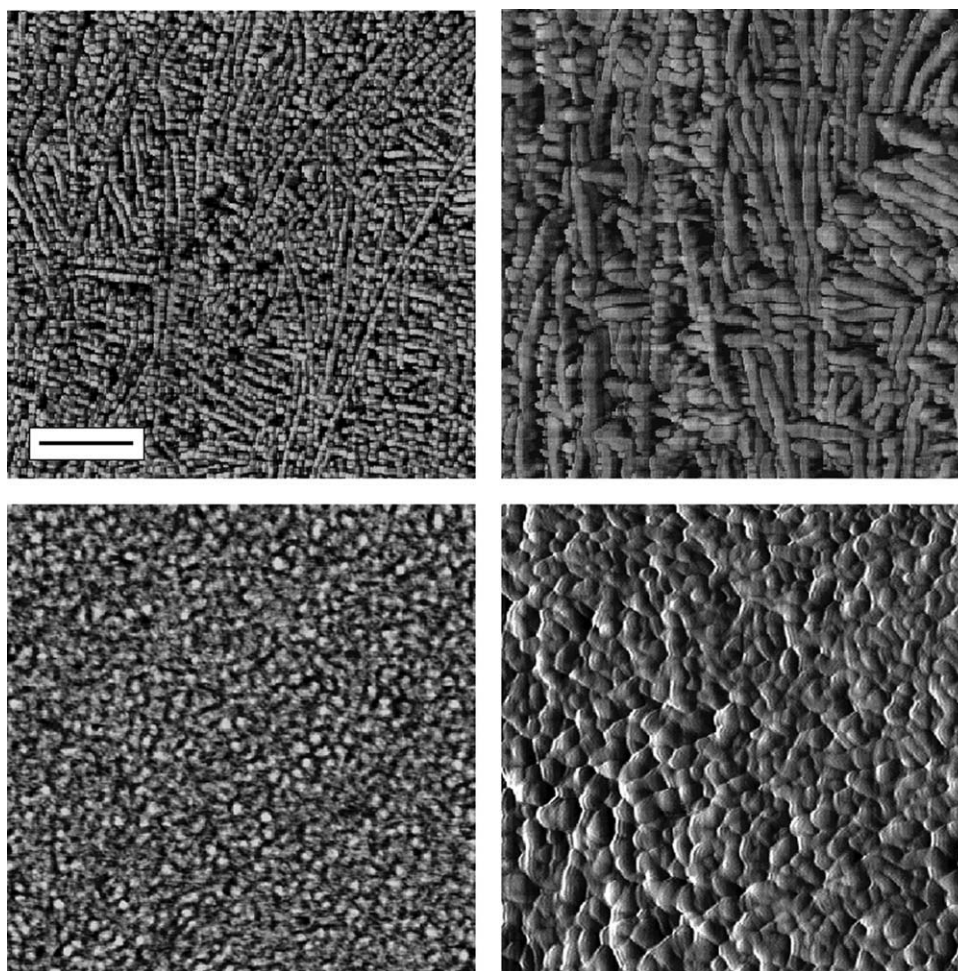


**Figure 2** Phase-mode AFM images of 100- $\mu\text{m}$ -thick iPP films melt-crystallized at 0.1 (top) or 450 K/s (bottom) before annealing (left) and after annealing at 433 K (right) for 60 min. The scale bar represents 200 nm.

spherulitic superstructure. The superstructure of selected preparations with a different history of crystallization was not affected, qualitatively or quantitatively, as result of annealing.

Figure 2 shows the phase-mode AFM images of the structure of spherulitic and nonspherulitic samples at the nanometer scale, with the scaling bar representing a distance of 200 nm. The top images were obtained on a spherulitic sample that initially was nonisothermally crystallized at a rate of 0.1 K/s, whereas the bottom images were collected on a nonspherulitic sample initially crystallized on rapid cooling at 450 K/s. The left images show the original structure after the specific primary crystallization step, and the right images show the structure after annealing at 433 K for a period of 60 min. Melt crystallization during cooling at a rate of 0.1 K/s led to the formation of laterally extended crosshatched lamellae with a thickness of about 10 nm. X-ray measurements confirmed the expected monoclinic structure of the crystals. As result of annealing at 433 K, the thickness of the lamellae increased to 26 nm. Rapid cooling at 450 K/s, in contrast, inhibited

the formation of lamellae and allowed only the formation of mesomorphic nodules with a size close to 15 nm. Subsequent heating and annealing at 433 K resulted in an increase in the size of nodules to about 35 nm and a change in the mesomorphic structure into a monoclinic structure by local rearrangement of the molecular segments.<sup>8,10</sup>

In summary, the images in Figures 1 and 2, together with unreported X-ray data, proved that iPP films of almost identical crystallinity but qualitatively different crystal habits and superstructures could be prepared. Rapid cooling, or crystallization at high supercooling, respectively, yielded mesomorphic or monoclinic nodules of adjustable size, which were not organized in spherulites. Crystallization at low supercooling, in contrast, led to the formation of lamellae arranged in spherulites.

#### Effect of the structure at the micrometer scale on the light transmission of the iPP films

Figure 3 shows the light transmission of nonisothermally (left graph) and isothermally (right graph)

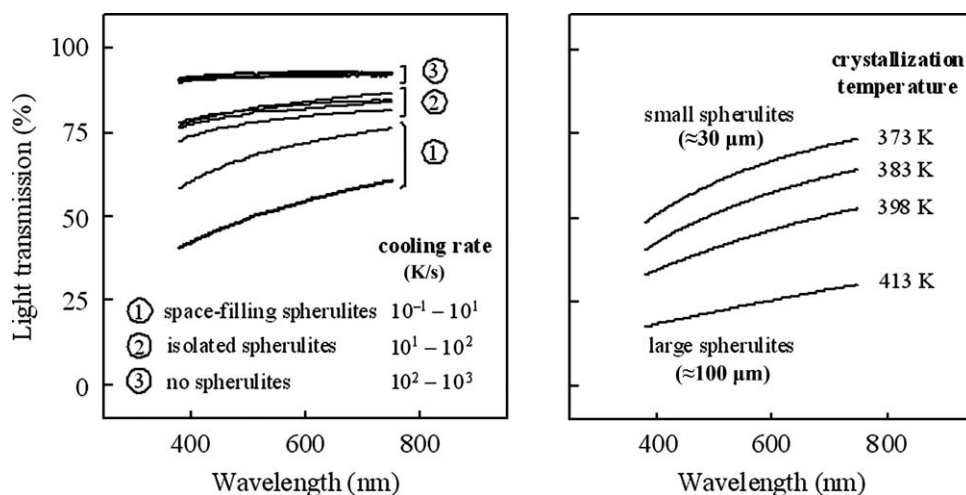


**Figure 3** Light transmission of 100- $\mu\text{m}$ -thick iPP films melt-crystallized nonisothermally (left) or isothermally (right) as a function of the wavelength.

melt-crystallized films of iPP as a function of wavelength. For the nonisothermally melt-crystallized samples, the light transmission spectrum shifted systematically to higher transmission values when the samples were crystallized at higher cooling rates. The light transmission was about 50% for films that were crystallized on cooling at a rate between  $10^{-1}$  and  $10^1$  K/s. The structures of these films at the various length scales are shown in Figures 1 and 2. These films were semicrystalline with the crystals exhibiting a lamellar shape and organized in spherulites. With decreasing size of spherulites, an increase in the light transmission was detected. Finally, the light transmission exceeded 90% when spherulites were completely absent, as was documented with the film crystallized at 450 K/s, despite the fact that the structure of this particular specimen was semicrystalline and heterogeneous at the nanometer scale. Additionally, we observed an increase in the light transmission with increasing wavelength. This effect was more pronounced in the spherulitic preparations. For instance, the light transmission of the sample that was melt-crystallized at 0.1 K/s (bottom thick line, Fig. 3) was close to 40% at a wavelength of 380 nm, whereas it was 60% at a wavelength of 750 nm. In contrast, the light transmission increased only slightly from 91 to 93% in the case of the sample initially melt-crystallized at a rate of cooling of 450 K/s (top thick line, Fig. 3).

A similar trend of an increase in the light transmission with decreasing size of spherulites was observed in the isothermally melt-crystallized iPP films. The presence of large spherulites with an average size of about 100  $\mu\text{m}$ , as was detected in the film melt-crystallized at a temperature of 413 K, led to extremely low values of the light transmission of only 17 and 30% at the low and high wavelength

limits of the measurement, respectively. In contrast, the light transmission of the specimen that was melt-crystallized at a temperature of about 373 K and that contained spherulites with a reduced size of only about 30  $\mu\text{m}$  showed a light transmission between 49 and 73%, with the larger value obtained at a higher wavelength.

It has been shown in previous studies<sup>8,17</sup> that the formation of spherulites in iPP is invariably connected with the formation of monoclinic lamellae and that the formation of a nonspherulitic superstructure preparation is connected with the formation of mesomorphic nodules. For this reason, the obtained different values of light transmission in the spherulitic and nonspherulitic films may also have been affected by the different structures at the nanometer scale, that is, by different sizes, habits, and structures of the crystals. To more precisely characterize the influence of these parameters on the light transmission of iPP, annealing experiments of selected preparations were performed that altered only the structure at the nanometer scale.

#### Effect of the structure at the nanometer scale on the light transmission of the iPP films

Figure 4 shows light transmission spectra of initially spherulitic (bottom three curves) and nonspherulitic (top three curves) preparations of iPP before and after annealing at 393 and 433 K. The spectra of the spherulitic and nonspherulitic preparations before and after annealing were not different; that is, the change in light transmission due to annealing was less than about 3%, which was the approximate experimental error. The annealing of nonspherulitic iPP, obtained by rapid cooling of the melt, led (1) to

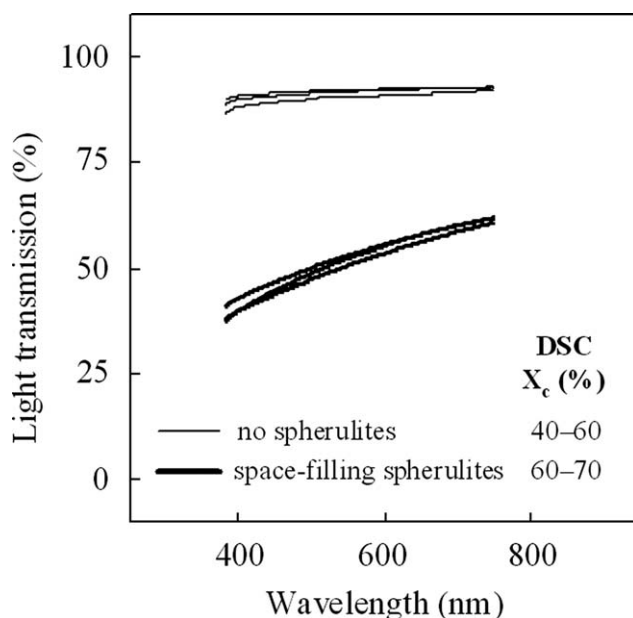


**Figure 4** Light transmission of 100- $\mu\text{m}$ -thick iPP films with a spherulitic superstructure or a nonspherulitic superstructure before and after annealing at 393 and 433 K ( $X_c$  = degree of crystallinity).

an increase in the enthalpy-based crystallinity from about 40 to 60%, (2) to a mesomorphic–monoclinic phase transition within the ordered phase, and (3) to a more than twofold increase in the size of crystals/domains from 15 to 35 nm without affecting their habit. All of these changes in the structure at the nanometer scale did not influence the optical transparency of the material because the UV–vis spectra were identical. Similarly, in the case of the spherulitic film prepared by isothermal crystallization at 0.1 K/s, annealing caused (1) a minor increase in the crystallinity from about 60 to 70% and (2) an increase in the thickness of the monoclinic lamellae from 10 to 26 nm. The structure at the micrometer scale was unchanged; that is, the size and number of spherulites remained constant. The light transmission was not affected by the increase in the crystallinity or by the increase in the lamellar thickness. Furthermore, we expected that the spherical aggregation of anisotropic lamellae resulted in an optically heterogeneous structure, which strongly decreased the light transmission with decreasing wavelength. It has been shown that an increased tendency of the orientation of lamellae, initially organized in a higher order spherulitic superstructure, for instance, by cold drawing, which also led to the destruction of spherulites, increased the transparency.<sup>28–30</sup> Similarly, the nonlamellar isometric crystals of iPP did not form a higher order superstructure, and therefore, a light transmission of about 90% was maintained within the investigated wavelength range.

#### Quantitative relation between the spherulite size and transparency

The data of Figures 1–4 led us to the conclusion that the light transmission in the iPP films was primarily controlled by the presence and size of the spherulites. The absence of spherulites decreased the light scattering, and consequently, the transparency was almost 100%. We did not observe indications about the influence of the crystallinity, crystal structure, or crystal morphology on the light transmission/transparency. The presence of spherulites was connected with light scattering, and the transparency decreased as a function of the size of the spherulites. The relation between the spherulite size in the iPP films and the transparency at a wavelength of 500 nm is quantified in Figure 5. The filled and open squares represent data that were obtained for isothermally and nonisothermally melt-crystallized samples, respectively, and the stars represent data obtained for annealed preparations. The encircling of data points illustrates the absent effect of annealing, that is, of absent changes in the structure at the nanometer scale on the light transmission. A minimum transparency of about 25% was observed for the iPP film with an average spherulite size of about 100  $\mu\text{m}$ . The transparency increased to about 75% when the size of spherulites decreased to about 20  $\mu\text{m}$ . The data obtained on the spherulitic samples with different histories of crystallization fit an almost linear

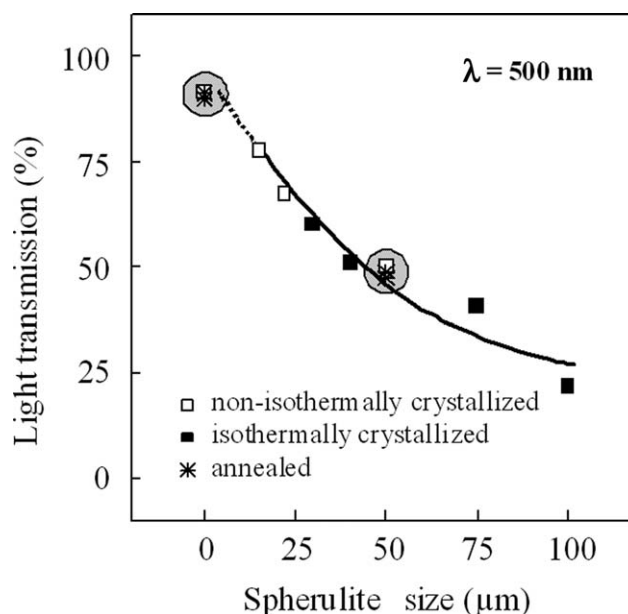


**Figure 5** Light transmission of 100- $\mu\text{m}$ -thick iPP films at a wavelength of 500 nm as a function of the size of the spherulites. The samples were melt-crystallized isothermally or nonisothermally and annealed at an elevated temperature. Data for samples of identical transparency but different crystallinities are circled.

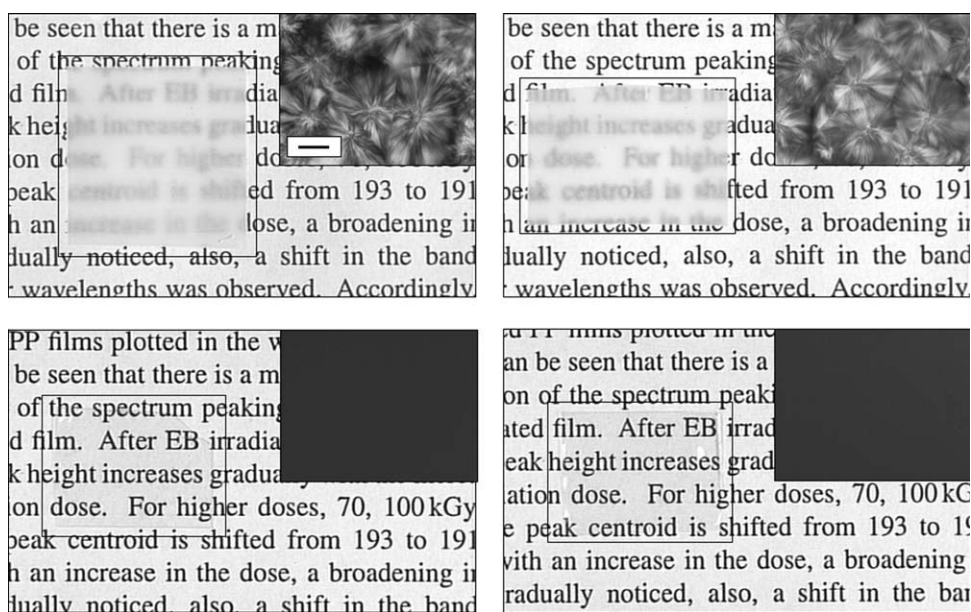


**Figure 6** See-through clarity and spherulitic superstructure of 100- $\mu\text{m}$ -thick iPP films initially melt-crystallized at 0.1 (top) or 450 K/s (bottom) before annealing (left) and after annealing at 433 K (right) for 60 min. Small rectangles have been drawn to identify the iPP films. The scale bar represents 20  $\mu\text{m}$ .

relationship; this indicated independence of transparency on the exact method of film preparation. In addition, extrapolation to zero spherulite size yielded a value that was experimentally obtained on the nonspherulitic preparations. The data of Figure 5 clearly showed that the transparency of the iPP films was primarily controlled by the size of the spherulites, where the loss of transparency due to light interaction with the internal structure of spherulites could not be neglected.

## CONCLUSIONS

In this study, we analyzed the effect of the structure, formed at the micrometer and nanometer scales, by controlled conditions of isothermal and nonisothermal crystallization on the light transmission of 100  $\mu\text{m}$  thick iPP films. The results of this study allowed us to establish a direct correlation between the size of spherulites and the light transmission. An increase in the light transmission with decreasing size of spherulites was detected. The light transmission finally approached a value close to 100% in the nonspherulitic samples. The transmission of visible light through the iPP films was not affected by the variation of crystallinity or the structure and size of the crystals. A higher see-through clarity in the iPP films was demonstrated by nonspherulitic preparations, as shown in Figure 6. The top films of low see-through clarity exhibited crystallinities of 60% (left) and 70% (right) and an average spherulite size of about 50  $\mu\text{m}$ . The bottom two nonspherulitic films

of high see-through clarity exhibited crystallinities of 40% (left) and 60% (right). The small rectangles in Figure 6 were drawn for better identification of the iPP films. It is possible to prepare films of identical transparency but of different crystallinity and crystal size, which impact the mechanical properties, such as modulus of elasticity and toughness.

The authors thank André Wutzler, Manfred Dubiel, and Christine Seidel at the Martin Luther University of Halle-Wittenberg for their kind assistance with the measurement of the UV-vis spectra.

## References

- Hsu, C. C.; Geil, P. H.; Miyaji, H.; Asai, K. *J Polym Sci Part B: Polym Phys* 1986, 24, 2379.
- Turner, A. J.; Aizlewood, J. M.; Beckett, D. R. *Makromol Chem* 1964, 75, 134.
- Caldas, V.; Brown, G. R.; Nohr, R. S.; MacDonald, J. G.; Raboin, L. E. *Polymer* 1994, 5, 899.
- Padden, F. J.; Keith, H. D. *J Appl Phys* 1959, 30, 1479.
- Norton, D. R.; Keller, A. *Polymer* 1985, 26, 704.
- Piccarolo, S. *J Macromol Sci Phys* 1992, 31, 501.
- De-Santis, F.; Adamovsky, S.; Titomanlio, G.; Schick, C. *Macromolecules* 2006, 39, 2562.
- Zia, Q.; Androsch, R.; Radosch, H. J.; Piccarolo, S. *Polymer* 2006, 47, 8163.
- Ogawa, T.; Miyaji, H.; Asai, K. *J Phys Soc Jpn* 1985, 54, 3668.
- Androsch, R. *Macromolecules* 2008, 41, 533.
- Zannetti, R.; Celotti, G.; Fichera, A.; Francesconi, R. *Makromol Chem* 1969, 128, 137.
- Zia, Q.; Radosch, H. J.; Androsch, R. *Polymer* 2007, 48, 3504.
- Zia, Q.; Mileva, D.; Androsch, R. *Macromolecules* 2008, 41, 8095.
- Bheda, J. H.; Spruiell, J. E. *Polym Eng Sci* 1986, 26, 736.

15. Mark, H. F.; Graylord, N. G.; Bikales, N. M. Encyclopedia of Polymer Science and Technology; Wiley: New York, 1968; Vol. 7.
16. Lin, Y. J.; Dias, P.; Chum, S.; Hiltner, A.; Baer, E. Polym Eng Sci 2007, 46, 1658.
17. Mileva, D.; Androsch, R.; Radusch, H. J. Polym Bull 2009, 62, 561.
18. Shibayama, M.; Imamura, K. I.; Katoh, K.; Nomura, S. J Appl Polym Sci 1991, 42, 1451.
19. Feng, Y.; Jin, X.; Hay, J. N. J Appl Polym Sci 1998, 69, 2089.
20. Losev, Y. P. Handbook of Engineering Polymeric Materials; CRC: Boca Raton, FL, 1997.
21. LyondellBasell Polymers. <http://www.basell.com> (accessed Oct 2009).
22. Androsch, R.; Wunderlich, B. Macromolecules 2001, 34, 5950.
23. Brucato, V.; Piccarolo, S.; La-Carruba, V. Chem Eng Sci 2002, 57, 4129.
24. Zia, Q.; Androsch, R.; Radusch, H. J.; Ingolič, E. Polym Bull 2008, 60, 791.
25. Brandrup, J.; Immergut, E. H. Polymer Handbook, 3rd ed.; Wiley: New York, 1989; Vol. 29.
26. Wunderlich, B. Thermal Analysis of Polymeric Materials; Springer: Berlin, 2004.
27. Mileva, D.; Zia, Q.; Androsch, R.; Radusch, H. J.; Piccarolo, S. Polymer 2009, 50, 5482.
28. Stein, R.; Prud'homme, R. E. J Polym Sci Polym Lett Ed 1971, 9, 595.
29. Pritchard, R. Plast Eng Trans 1964, 4, 66.
30. Stein, R. S.; Rhodes, M. B. J Appl Phys 1960, 31, 1873.